Left-Handed Dimer of EphA2 Transmembrane Domain: Helix Packing Diversity among Receptor Tyrosine Kinases

Eduard V. Bocharov,[†] Maxim L. Mayzel,[†] Pavel E. Volynsky,[†] Konstantin S. Mineev,[†] Elena N. Tkach,[‡] Yaroslav S. Ermolyuk,[‡] Alexey A. Schulga,[‡] Roman G. Efremov,[†*] and Alexander S. Arseniev[†]
[†]Division of Structural Biology and [‡]Division of Protein Engineering, Shemyakin-Ovchinnikov Institute of Bioorganic Chemistry RAS, Moscow, Russia

ABSTRACT The Eph receptor tyrosine kinases and their membrane-bound ephrin ligands control a diverse array of cell-cell interactions in the developing and adult organisms. During signal transduction across plasma membrane, Eph receptors, like other receptor tyrosine kinases, are involved in lateral dimerization and subsequent oligomerization presumably with proper assembly of their single-span transmembrane domains. Spatial structure of dimeric transmembrane domain of EphA2 receptor embedded into lipid bicelle was obtained by solution NMR, showing a left-handed parallel packing of the transmembrane helices $(535–559)_2$. The helices interact through the extended heptad repeat motif $L^{535}X_3G^{539}X_2A^{542}X_3V^{546}X_2L^{549}$ assisted by intermolecular stacking interactions of aromatic rings of $(FF^{557})_2$, whereas the characteristic tandem GG4-like motif $A^{536}X_3G^{540}X_3G^{544}$ is not used, enabling another mode of helix-helix association. Importantly, a similar motif AX_3GX_3G as was found is responsible for right-handed dimerization of transmembrane domain of the EphA1 receptor. These findings serve as an instructive example of the diversity of transmembrane domain formation within the same family of protein kinases and seem to favor the assumption that the so-called rotation-coupled activation mechanism may take place during the Eph receptor signaling. A possible role of membrane lipid rafts in relation to Eph transmembrane domain oligomerization and Eph signal transduction was also discussed.

INTRODUCTION

Signaling by Eph receptor tyrosine kinases and their cognate ephrin ligands forms an essential part of a highly conserved molecular mechanism coordinating cell migration and positioning in human organism (1,2). Intensive investigation of the expression of Eph receptors and ephrins in various adult and embryonic tissues and of their role in different physiological processes in norma and pathology has begun only recently (3). Because all Eph receptors and ephrins are cell surface-associated proteins, a direct cell-cell contact is required for receptor activation resulting in cytoskeletal remodeling that underlies cell adhesion, repulsion and motility in both communicating cells. Based on sequence conservation, binding activity, and the mode of membrane attachment for ephrin, Eph receptors and ephrins are divided into two subclasses, A and B (4). Similar to other receptor tyrosine kinases, extracellular ligand-binding domain and cytoplasmic tyrosine kinase domains of the Eph receptors from both subclasses EphA and EphB are connected by a single TM helix. The extracellular receptor-binding domain of the ephrin ligands is tethered to the cell surface by either a glycosyl-phosphatidyl-inositol anchor (ephrinA) or a single TM helix followed by a C-terminal cytoplasmic domain (ephrinB). Whereas ligand binding to other receptor tyrosine kinases induces signaling only the receptor-bearing cell, the ephrin-Eph binding triggers bidirectional signaling (reverse and forward) in both receptor-bearing cell and the ligand-presenting cell (1,2). Before cell-cell contact, it is thought that both ephrins and Eph receptors are loosely preclustered in lipid rafts and can form low-affinity ephrin-ephrin and Eph-Eph dimers (5–7) that may be widespread among receptor tyrosine kinases (8,9). In contrast to other receptor tyrosine kinases activated by proper ligand-induced dimerization or by reorientation of monomers in preformed receptor dimers (8,10,11), the ligand binding additionally stimulates formation of large ephrin-Eph signaling clusters within respective plasma membrane (2,12,13). Thus, depending on the oligomerization state of ephrin-Eph receptor signaling complexes, distinct biological effects can be induced. Besides high-affinity ephrin-binding interface, several sites contributing to initial dimerization and further low-affinity oligomerization were identified in the Eph extracellular and cytoplasmic domains (2,12,13). Whereas the specific interactions of single TM spanning domains were recognized to assist the ligand-binding extracellular domains during activation of some receptor tyrosine kinases (10,11,14,15), functional role of the TM domains in the Eph receptor association still remained unclear.

We obtained recently a high-resolution structure for the right-handed homodimeric TM domain of human receptor EphA1 in membrane mimicking environment and identified a pH-induced realignment of the helix packing in the dimer presumably between the two characteristic dimerization motifs (16). Identification of several characteristic

Submitted August 5, 2009, and accepted for publication November 6, 2009.

*Correspondence: efremov@nmr.ru

Abbreviations used: DHPC, dihexanoyl-phosphatidylcholine; DMPC, dimyristoyl-phosphatidylcholine; DPPC, dipalmitoyl-phosphatidylcholine; Eph, erythropoietin-producing hepatocellular; HSQC, heteronuclear single quantum coherence; MD, molecular dynamics; MHP, molecular hydrophobicity potential; NOE, nuclear Overhauser effect; NOESY, NOE spectroscopy; TM, transmembrane; TOCSY, total correlation spectroscopy.

Editor: Mark Girvin.

0006-3495/10/03/0881/9 $2.00

doi: 10.1016/j.bpj.2009.11.008

dimerization motifs in the TM sequence of the Eph receptor suggests the ability of its TM domains to associate diversely in plasma membrane, and thus to participate directly in the ligand-independent and/or ligand-induced dimerization and clustering of the Eph receptor. Here we describe the high-resolution NMR structure of the left-handed homodimeric TM domain of human receptor EphA2 embedded into lipid bicelles, providing the evidence that TM domains of the Eph receptors can self-associate in a different manner. This serves as an instructive example of the diversity of TM domain formation within the same family of receptor protein kinases and implies the so-called rotation-coupled activation mechanism (10,11) of the receptor. Also, it should be noted that EphA2 is the first single-spanning membrane receptor whose noncovalent left-handed dimeric structure of the TM domain has been determined experimentally.

Aberrant activity of EphA2 widely expressed in normal human tissues has been implicated in numerous human pathological states, especially in cancer development (17,18). The clinical significance of EphA2 was observed in breast, prostate, colon, skin, cervical, ovarian, bladder, and lung cancers. We believe that investigation of the structural-dynamic properties of the EphA2 TM domain would supply a basis to control the receptor kinase activity in pathological states of the organism.

MATERIALS AND METHODS

NMR sample preparation and optical characterization

Recombinant human EphA2 fragment 523–563 (EphA2tm) was produced in bacteria and purified as described in the Supporting Material. Three EphA2tm samples were prepared: uniformly $^{15}N/^{13}C$-labeled, ^{15}N-labeled, and a 1:1 mixture of uniformly $^{15}N/^{13}C$-labeled and unlabeled proteins (''heterodimer'' sample). The 1 mM samples of EphA2tm were incorporated into 1:4 DMPC/DHPC lipid bicelles (with a lipid/protein molar ratio of 35) at pH 5.0 in a buffer solution containing 20 mM deuterated sodium acetate, 0.15 μM sodium azide, 1 mM EDTA, and 5% D_2O. The lipids having deuterated hydrophobic tails were used. The deuterated 1,2-di-[$^2H_{27}$]-myristoyl-*sn*-glycero-3-phosphocholine (d_{54}-DMPC) and 1,2-di-[$^2H_{11}$]-myristoyl-*sn*-glycero-3-phosphocholine (d_{22}-DHPC) were synthesized from *sn*-glycero-3-phosphocholine by acylation with anhydride of d_{27}-myristic acid and d_{11}-hexanoic acid, respectively, as described (19). First, EphA2tm was dissolved in water/trifluoroethanol 1:1 at room temperature, and then NMR samples were prepared by adding of DMPC/DHPC (also in water/trifluoroethanol mixture), lyophilizing and dissolving with the water buffer. Before structural studies, the samples were subjected to several freeze/thaw cycles for the achievement of uniform protein distribution among the lipid bicelles. An Eppendorf containing the NMR sample was frozen into ethanol bath (−20°C) and kept at the room temperature ~10 min. The five freeze/thaw cycles were usually carried out with slightly sonication of the samples at each cycle up to obtaining a clear solution and good NMR spectra. To verify the validity of NMR experimental conditions, dynamic light scattering (DynaPro Titan instrument; Wyatt Technology, Santa Barbara, CA) and circular dichroism (JASCO-810 spectropolarimeter; Jasco, Tokyo, Japan) studies were carried out.

NMR spectroscopy and structure determination

NMR spectra were acquired at 40°C on 600-MHz (^1H) Unity spectrometer (Varian, Palo Alto, CA) equipped with a pulsed-field gradient unit and a triple-resonance probe. The backbone and side chain ^1H, ^{13}C, and ^{15}N resonances of EphA2tm were assigned using standard triple-resonance techniques (20,21). Two- and three-dimensional ^1H-^{15}N and ^1H-^{13}C HSQC, ^{15}N-edited TOCSY (40-ms mixing time), HNCA, HN(CO)CA, HNCACB, and CBCA(CO)NH spectra in H_2O provided backbone and partial side chain assignments, whereas HCCH-TOCSY (15.6-ms and 23.4-ms mixing times) and ^1H NOESY experiments in D_2O facilitated side chain assignments. Resonance assignments were carried out with the CARA software (22).

The values of heteronuclear $^{15}N\{^1H\}$ steady-state NOE, ^{15}N longitudinal (T_1), and transverse (T_2) relaxation times were obtained for the ^{15}N-labeled sample as described in the Supporting Material. The local effective rotation correlation times (τ_R) for the individual ^{15}NH groups were calculated from the T_1/T_2 ratio using the DASHA software (23). Effective molecular mass of the EphA2tm dimer embedded into the DMPC/DHPC bicelle was estimated according to the empirical dependence (24) from overall rotation correlation time averaged over ^{15}NH groups with $^1H\{^{15}N\}$ NOE > 0.6 and without noticeable crosspeak broadening in ^1H-^{15}N HSQC spectra.

NMR spatial structures of the EphA2tm dimer were calculated using the CYANA program (25). Intramonomeric NOE distance restraints were identified with CARA through the analysis of 3D ^{15}N- and ^{13}C-edited NOESY-HSQC (60- and 80-ms mixing times) spectra (21) obtained for ^{15}N- and $^{15}N/^{13}C$-labeled samples in H_2O and D_2O, respectively. The 2D ^1H NOESY (80-ms mixing time) spectrum acquired for the unlabeled sample was used as an additional source of structural information concerning aromatic ring protons. Intermonomeric distance restraints were derived from 3D ^{13}C F1-filtered/F3-edited-NOESY spectrum (26) acquired with a 80-ms mixing time for the heterodimer sample in D_2O. To reduce the effect of different magnetic relaxation rates, resulting in segregation of crosspeaks intensities during the NMR pulse sequence, the different calibration constants was used for the calibration of intermonomeric NOE crosspeaks observed in the 3D ^{13}C F1-filtered/F3-edited-NOESY spectrum between methyl groups and methyl, methylene, and backbone protons. The calibration constants were based on the restraints determined for reference unambiguously intermonomeric crosspeaks belonging to the corresponding classes in 3D ^{13}C-edited-NOESY spectrum, Additionally, the ''artifact'' crosspeaks, which appear due to imperfection of the heteronuclear filter and of ^{13}C-labeling of protein, were monitored using 3D ^{13}C F1-filtered/F3-edited-NOESY spectrum acquired for the $^{15}N/^{13}C$-labeled sample of the EphA2tm dimer. Also, during the structure calculation, in the case of distance restrains for pseudoatoms representing groups with several protons, the sum of reversed sixth power of possible proton-proton distances was made to be less than reversed sixth power of total distance limit for the pseudoatom crosspeak. Stereospecific assignments and torsion angle restraints for φ, ψ, and χ^1 were obtained by the analysis of local conformation in CYANA using sequential NOE data and the available $^3J_{HN\alpha}$ and $^3J_{N\beta}$ coupling constants evaluated qualitatively from 3D ^1H-^{15}N HNHA and ^1H-^{15}N HNHB experiments (21). Backbone dihedral angle restraints were also estimated based on the assigned chemical shifts using the TALOS program (27). Slowly hydrogen-deuterium exchanging amide groups were identified by reconstituting lyophilized $^{15}N/^{13}C$-labeled sample in D_2O and recording a series of ^1H-^{15}N HSQC spectra over one week. Taking into account the ^{15}N relaxation data, the slowly exchanging amide protons were assigned as donors of backbone hydrogen bonds with related hydrogen-acceptor partners on the basis of preliminary structure calculations. The EphA2tm dimer was modeled as a complex of two EphA2tm fragments linked by twenty pseudo-residues to give the monomers enough space for mutual arrangement. The standard CYANA simulated annealing protocol was applied to 100 random structures using the angle and distance restraints symmetrically doubled for each dimer subunit, and resulting 15 NMR structures of the EphA2tm dimer with the lowest target function were selected.

Restrained energy relaxation of the representative NMR structures of the EphA2tm dimer was carried out by MD in hydrated explicit DMPC and DPPC bilayers using the GROMACS 3.3.1 package (28). Construction of the protein/lipid system and MD protocol are described in the Supporting Material. 6-ns MD runs for the representative models of the EphA2tm dimer were carried out with the NMR-derived intra- and intermonomeric distance

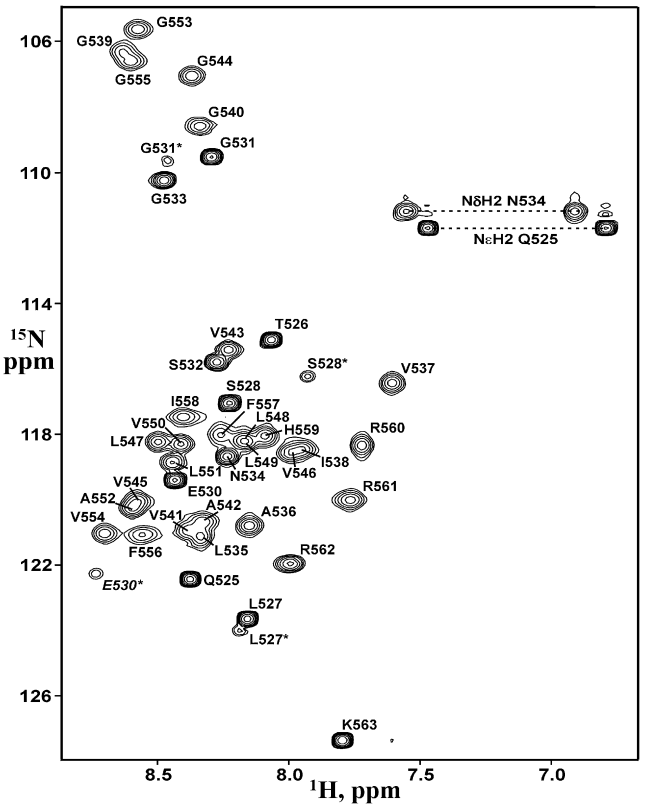

FIGURE 1 NMR spectrum of the EphA2tm dimer embedded into lipid bicelles. The ^{1}H-^{15}N HSQC spectrum of 1 mM ^{15}N-labeled EphA2tm in DMPC/DHPC (1/4) bicelles at 40°C and pH 5.0. The ^{1}H-^{15}N backbone resonance assignments are shown. The amide crosspeaks of solvent-exposed N-terminal residues have a minor component (marked by asterisk) due to slow *cis*/*trans* transitions of Ser^{528}-Pro^{529} peptide bond in the flexible N-terminal part of EphA2tm.

restraints. To check the stability of the resulting systems, 2-ns continuations of the MD runs were carried out without distance restraints. Equilibrium parts of MD trajectories (last 2 ns) were analyzed using home made software and utilities supplied with the GROMACS package.

TM regions of Eph receptors were predicted with TMpred (29). Hydrophobic properties of α-helices were calculated using the MHP approach (see the Supporting Material for details) (30). The contact area between the dimer subunits was calculated using the DSSP program (31) as a difference between the accessible surface areas of EphA2tm residues in the monomer and dimer. The EphA2tm structures were visualized with MOLMOL (32) and PYMOL (33).

RESULTS

Validation of NMR sample conditions for EphA2 TM domain in membrane mimicking environment

To investigate the structural and dynamic behavior of TM domain of the EphA2 receptor tyrosine kinase in a membrane mimicking environment, a recombinant 41-residue EphA2 fragment 523–563 (named EphA2tm) with the sequence EFQTLSPEGSGNLAVIGGVAVGVVLLLVLAGVGFFIH RRRK, including predicted hydrophobic TM segment (underlined) flanked by polar N- and C-terminal regions, was prepared. Though different membrane mimicking systems have been used to investigate membrane-bound proteins, so far discoidal mixed bicelles composed of a small circular bilayer of long-chain lipids surrounded by a rim of short-chain lipids have proved more suitable for structural studies by high-resolution NMR (for review see Prosser et al. 34). Indeed, our recent experiences of resolving the dimeric structures of TM domains of human proteins, including the EphA1 receptor, allow stating that bicelles are a fairly adequate model of lipid membrane (16,35,36). Therefore, the recombinant ^{15}N and ^{13}C isotope labeled EphA2tm samples were studied by heteronuclear NMR technique in an aqueous suspension of DMPC/DHPC (1/4) bicelles. The prepared sample solutions were clear, and preliminary NMR spectra (Fig. 1) seen rather suitable for structural studies. Circular dichroism spectrum, recorded to validate the NMR experimental conditions, reveals an α-helical structure (~63%) of EphA2tm in the membrane mimetic (see Fig. S1 *A* in the Supporting Material). Dynamic light scattering showed that the EphA2tm bicellar sample is monodisperse, practically containing only one type of particles with hydrodynamic radius of 25 $\pm$ 2 Å (Fig. S1 *B*) typical for such bicelles (37,38). The observed protein-lipid NOE contacts (Fig. 2 *B* and Fig. S3, *B* and *C*) and location of slowly hydrogen-deuterium exchanging amide groups (Fig. 2 *D*) indicate that EphA2tm is integrated into lipid bicelle. The measured ^{15}N{^{1}H} NOE (Fig. 2 *F*), ^{15}N T_1 and T_2 values (Fig. S2) and calculated effective rotation correlation times τ_R (Fig. 2 *G*) are indicative of a relatively rigid TM segment 535–559 flanked by highly flexible N- and C-terminal regions accessible to water, as shown by water exchange peaks observed in the ^{15}N-edited NOESY- and TOCSY-HSQC spectra (Fig. 2 *C*). Overall rotation correlation time estimated from T_1/T_2 ratio on the TM region is 14.5 ns that nearly corresponds to the molecular weight (~44 kDa) of the EphA2tm dimer surrounded by ~70 lipid molecules.

Dimerization pattern and spatial structure of the EphA2 TM domain in lipid bicelles

The unique set of intra- and intermonomeric NOE contacts (Fig. 2 *A* and Fig. S3, *A* and *B*) directly demonstrated that EphA2tm forms a dimer with parallel α-helical subunits symmetrical on the NMR timescale. Therefore, the NMR-derived dihedral angle restraints and both intra- and intermonomeric (Table S1) distance restraints were assigned for each dimer subunit that resulted in a dimer symmetrical over the ensemble of calculated structures (Fig. 3 *A*). A survey of the structural statistics for the final ensemble of the 15 NMR-derived structures of the EphA2tm dimer is provided in Table 1. The chemical shift assignments and atomic coordinates have been deposited in Biological Magnetic Resonance Data Bank (BMRB: 16005) and Protein Data Bank (PDB: 2k9y).

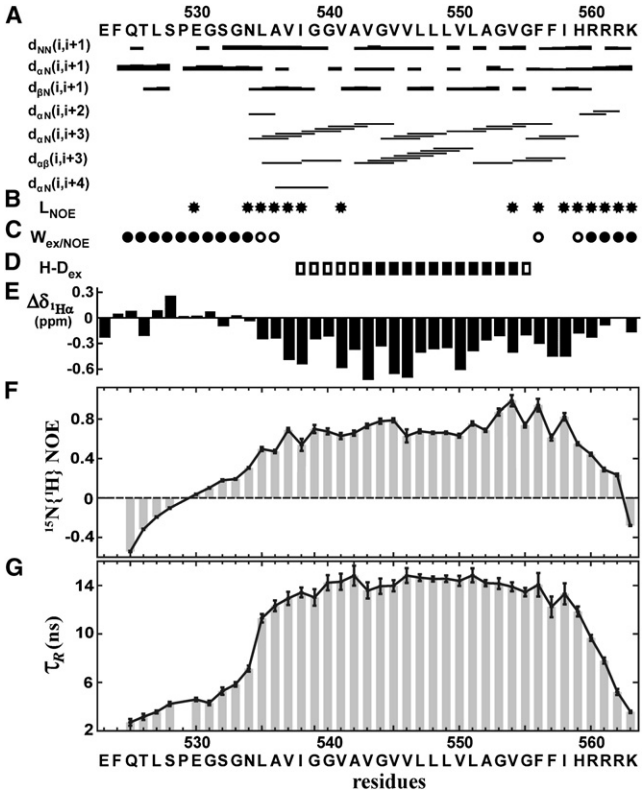

FIGURE 2 NMR data for the EphA2tm dimer embedded into lipid bicelles. (*A*) Intramonomeric sequential and medium range NOE connectivity observed in 3D ^{15}N- and ^{13}C-edited NOESY-HSQC spectra (80 ms mixing time) are shown by horizontal lines. The line thickness for the NOE connectivity is inversely proportional to the squared upper distance bound. The NOE information on some regions was restricted due to cross-peak broadening and overlapping. (*B*) The residues (*solid stars*) showing NOE contacts between their side chains and polar lipid heads. (*C*) Strong (*solid circle*) and weak (*open circle*) crosspeaks detected on the water frequency for the EphA2tm amide groups in the ^{15}N-edited NOESY- and TOCSY-HSQC spectra. The crosspeaks result from direct NOE, exchange-relayed NOE or chemical exchange (21) of the amide protons with water and anyway indicate water accessibility of the EphA2tm residue. (*D*) Slowly hydrogen-deuterium exchanging amide groups in the EphA2tm dimer according to estimated half-exchange times (40°C, pH 5.0): $0.5 < t_{1/2} < 4$ h (*open box*); $t_{1/2} > 4$ h (*solid box*). The data for the Phe^{556}, Phe^{557}, and Ile^{558} residues subjected to HN resonance broadening were not obtained. (*E*) ^{1}Hα secondary chemical shifts $\Delta\delta$ for the EphA2tm residues given by the difference between actual chemical shift and typical random-coil chemical shift for a given residue. Pronounced negative ^{1}Hα secondary chemical shifts indicate a helical structure of the protein (21). (*F*) Steady-state ^{15}N$\{^1$H$\}$ NOE for the backbone ^{15}N nuclei of the EphA2tm dimer. Uncertainties are shown by bars. (*G*) Effective rotation correlation times τ_R for the EphA2tm amide groups calculated from the ratio of ^{15}N longitudinal T_1 and transverse T_2 relaxation times (Fig. S2).

The membrane-spanning α-helices (residues 535–559) of EphA2tm cross at the angle θ of ~15° with the distance d of ~8 Å between helix axes, forming a left-handed parallel dimer, whereas the flexible N- and C-terminal regions flanking the TM segment are unfolded. The contact area between the TM helices of the EphA2tm dimer includes Leu^{535}, Ala^{536}, Ile^{538}, Gly^{539}, Ala^{542}, Val^{543}, Val^{545}, Val^{546}, Leu^{549}, Val^{550}, Phe^{556}, and Phe^{557} residues located along the entire TM helix (Fig. 3, *D–F*, and Fig. S4). The weekly polar N-terminal part of the EphA2tm dimer is tightly packed mainly owing to small Ala^{536}, Gly^{539}, and Ala^{542} residues interacting with the opposite side chains of Leu^{535}, Ile^{538}, and Val^{543} residues. In the center, the EphA2tm dimer is stabilized by intermonomeric contacts of the side chains of Val^{543}, Val^{545}, Val^{546}, Leu^{549}, and Val^{550} residues, forming a hydrophobic cluster flanked by a patch comprising Phe^{556} and Phe^{557} aromatic rings and Arg^{560} guanidino groups participating in multiple intra- and intermolecular π-π and π-cation interactions, which seem to be essential for proper helix alignment. The C-terminal part of the dimeric interface is not compact, so a weekly polar cavity formed by the backbone of Gly^{553} and Val^{554} residues and covered by the *Phe*-ring patch is remained between dimer subunits. Thus, being embedded into the DMPC/DHPC bicelles, the EphA2tm helices self-associate through the extended dimerization pattern $L^{535}X_3G^{539}X_2A^{542}X_3V^{546}X_2L^{549}X_7FF^{557}$, involving a heptad repeat zipper motif (analogous to ''leucine zipper'' motif but more polar) inherent to left-handed helix-helix interactions with small crossing angles stabilized by ''knobs-into-holes'' packing (39).

The representative NMR structures of the EphA2tm dimer were treated via energy relaxation by restrained MD in the explicit hydrated DMPC bilayer with imposition of NMR-derived distance restraints to adapt them to the membrane and to improve helix packing. It was found, that even for the restrained part of the MD trajectory the structures are subjected to considerable deformations accompanied by large tilt angle between dimer axis and normal to the bilayer (~30°) and partial exposure of the C-terminal phenylalanine aromatic rings to bulk water (Fig. S5 *A*). This is due to the so-called hydrophobic mismatch (40,41) causing instability of the identified dimeric structure of EphA2tm in the thin DMPC membrane (~34 Å as determined by phosphorus atoms), and removal of the NMR-derived restraints finally results in the helix dissociation. To overcome this, we prepared explicit hydrated DPPC bilayer, which is ~4 Å thicker (42). A subsequent round of energy relaxation did not cause considerable changes in the secondary and overall structure of the EphA2tm dimer, indicating its relative stability in the DPPC bilayer, in which the tilt angle of the dimer was decreased (Fig. 3 *B*).

Local conformational exchange near the *Phe*-ring patch and water penetration into the EphA2tm dimer interface

The experimental results showed that certain degree of conformational mobility exists in the interfacial region of the EphA2tm dimer, where intermonomeric stacking interactions occur in the group of four phenylalanine residues (Phe^{556}/Phe^{557})$_2$ forming a labile *Phe*-ring hydrophobic patch (Fig. 3, *B* and *C*). The ^{15}NH crosspeak broadening

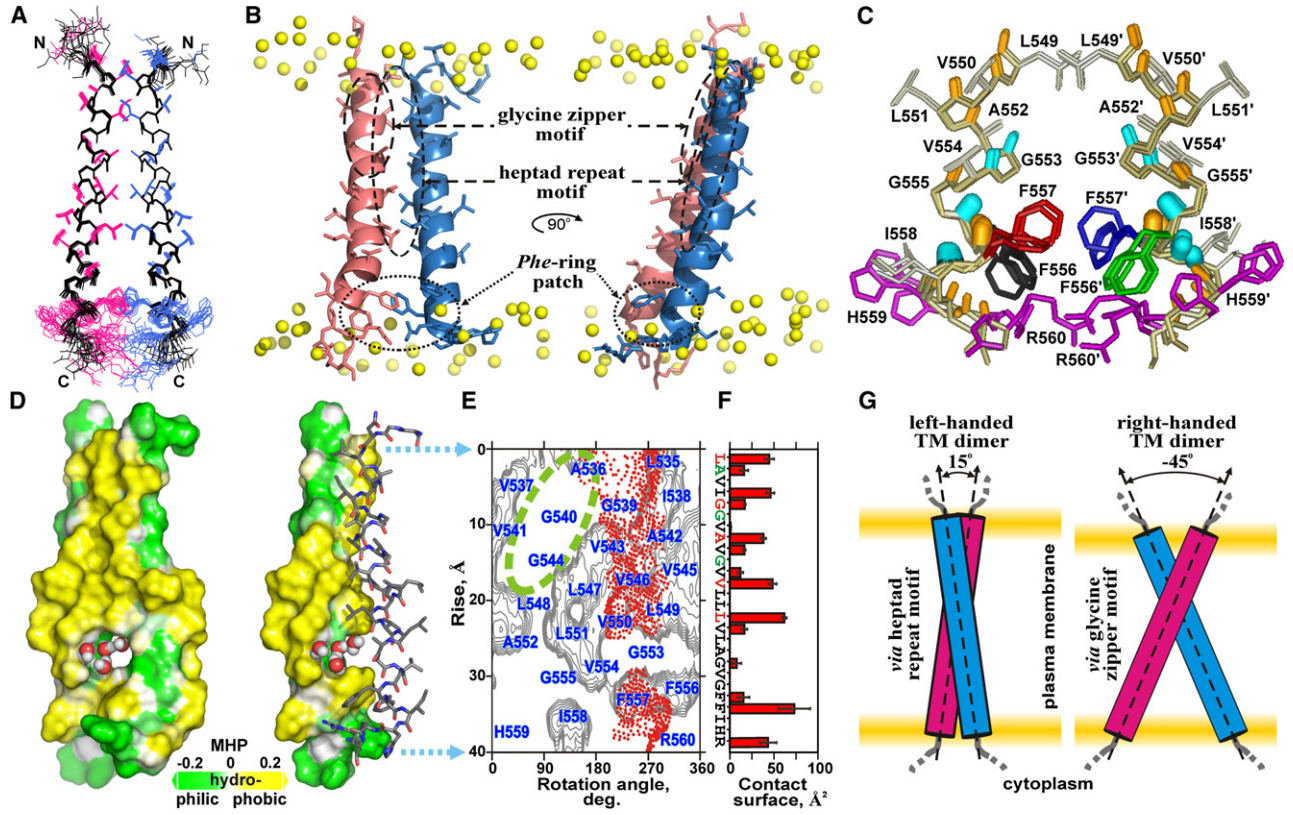

FIGURE 3 Spatial structure of the EphA2tm dimer. (*A*) Ensemble of 15 NMR-derived structures of the EphA2tm dimer after superposition of the backbone atoms of residues $(535–559)_2$ of both dimer subunits. Side chain (in *red* and *blue* for different monomers) and backbone (in *black*) heavy atom bonds of residues $(532–562)_2$ are shown. The EphA2tm dimer structure is presented in detail on Fig. S4. (*B*) Ribbon diagrams of the EphA2tm dimer relaxed in the explicit DPPC bilayer. Yellow balls show phosphorus atoms of lipid heads. Spatial locations of the two dimerization motifs, heptad repeat motif $L^{535}X_3G^{539}X_2A^{542}X_3V^{546}X_2L^{549}$ used in the EphA2tm dimerization and the potential N-terminal tandem GG4-like (glycine zipper) motif $A^{536}X_3G^{540}X_3G^{544}$, are marked by dashed ovals. *Phe*-ring patch composed of $(FF^{557})_2$ in the C-terminal part of the EphA2tm dimer interface is also highlighted. (*C*) Local conformational exchange near the *Phe*-ring patch (also see Fig. S6). Side chains of Phe^{556}, Phe^{557}, $Phe^{556'}$, and $Phe^{557'}$ of the EphA2tm dimer subunits from the three representative NMR structures are colored in black, red, green, and blue, respectively. Side chains of histidine and arginine residues are colored in purple. Amide groups of Gly^{553}, Val^{554}, Phe^{556}, and Ile^{558} having $^1H\{^{15}N\}$ NOE > 0.8 are highlighted in cyan. Amide groups of Phe^{556}, Phe^{557}, and Ile^{558} subjected to resonance broadening are presented by thick cylinders. (*D*) Hydrophobic and hydrophilic (polar) surfaces of TM helices of the EphA2tm dimer colored in yellow and green according to the MHP. Four water molecules penetrating into the weekly polar cavity located in the dimeric interface are shown. (*E*) Hydrophobicity map for the EphA2tm helix surface with contour isolines encircling hydrophobic regions with high values of MHP. Details about map construction are presented in the Supporting Material. The EphA2tm helix packing interface is indicated by red-point area. The potential dimerization glycine zipper motif is marked by dashed green oval. (*F*) TM helix packing contact surface per EphA2tm residue. The heptad repeat and glycine zipper motifs are highlighted in red and green, respectively. (*G*) Schematic illustration of membrane thickness preference of the EphA2 TM domain on dimerization via heptad repeat or glycine zipper motifs resulting in the left- or right-handed conformations, respectively, with different overall dimer shape.

(mainly on ^1H chemical shift direction) of Phe^{556}, Phe^{557}, and Ile^{558} in the ^1H-^{15}N HSQC spectrum (Fig. 1) indicates the presence of a conformational exchange in micro-millisecond timescale in the dimeric interface. Signal broadening and disproportional doubling (at least) are observed also for the aromatic rings of these residues, more pronouncedly for Phe^{557} (see ^1H-^{13}C HSQC spectrum in Fig. S6 *A*). According to a bifacial pattern of the local NOE contacts and the representative NMR structure set of the EphA2tm dimer, aromatic rings of Phe^{556} and Phe^{557} participate in intermolecular π-π interactions of different geometrical configurations, a combination from offset stacking to edge-face stacking, due to switching between *gauche*+ and *trans* rotamers of Cα-Cβ bond of Phe^{557} (Fig. 3 *C* and Fig. S6 *C*).

Intra- and intermolecular π-cation interactions of Arg^{560} guanidino groups with both Phe^{556} and Phe^{557} aromatic rings flank the EphA2tm dimer interface at the lipid head level. As shown by intramonomeric NOE contacts, secondary chemical shift values and ^{15}N relaxation data (Fig. 2), the EphA2tm C-terminal region 559–562 undergoes fast helix-coil transitions (on pico-nanosecond timescale) probably owing to repulsion between the positively charged side chains of Arg^{560}, Arg^{561}, and Arg^{562} (located in mutual proximity near the dimer interface) and their transient interactions with polar heads of lipids. Indeed, arginine and lysine residues have high helix propensity at the C-terminal end of TM helix, compensating interaction with the helix dipole, but they also have a tendency to participate in direct or

TABLE 1 Structural statistics for the ensemble of 15 best NMR structures of the EphA2tm dimer

NMR structure	Statistic
NMR distance and dihedral restraints	
Total unambiguous NOE restraints	724
Intraresidue	390
Interresidue	286
Sequential ($\|i-j\|=1$)	164
Medium-range ($1<\|i-j\|\leq 4$)	122
Long-range ($\|i-j\|>4$)	0
Intermonomeric	48
Hydrogen bond restraints (upper/lower)	120/120
Total torsion angle restraints	108
Backbone φ	34
Backbone ψ	32
Side chain χ^1	52
Structure calculation statistics	
CYANA target function (Å^2)	0.76 ± 0.17
Restraint violations	
Distance (>0.2 Å)	0
Dihedral (>5 Å)	0
Average pairwise RMSD (Å)	
Stable α-helical region $(535–559)_2$	
Backbone atoms	0.41 ± 0.14
All heavy atoms	0.86 ± 0.24
Ramachandran analysis*	
Residues in most favored regions (%)	79.6
Residues in additional allowed regions (%)	17.7
Residues in generously allowed regions (%)	2.4†
Residues in disallowed regions (%)	0.3†
Helix-helix packing	
Helix-helix contact surface (Å^2)	490 ± 30
Angle θ (deg.) between the TM helix axes	14 ± 2
Distance d (Å) between the TM helix axes	7.9 ± 0.2

*Ramachandran statistics was determined using CYANA (25).
†Residues from unfolded and flexible regions.

water-mediated polar–polar interactions with phospholipid headgroups or the glycerol backbone (43). In addition, as monitored by pH-dependence for chemical shifts (Fig. S7), deprotonation of His^{559} imidazole group (pK_a 5.6) on the C-terminus of the TM helix apparently leads to some local rearrangements of the water exposed C-terminal arginine residues due to appearance of additional π-cation interaction between the imidazole and guanidino side chain groups, whereas the EphA2tm dimer interface remains practically unaffected.

The experimentally identified switching of the π-π and π-cation interactions was evinced by MD relaxation of representative NMR structures of the EphA2tm dimer. Depending on an initial *Phe*-ring patch configurations, a switching between side chain rotamers of Phe^{557} accompanied by varied intra- and intermolecular interactions of Phe^{556}, Phe^{557}, Arg^{560}, and (occasionally) Arg^{561} was observed along the MD relaxation trace (Fig. S6 *D*). In addition, weak polar intra- and intermolecular interactions between the Gly^{553} and Val^{554} backbone atoms and the Phe^{557} aromatic rings also occur, supporting an observation that association of TM helices is enhanced by the proximity of phenylalanine and glycine residues (44). Thus, the MD relaxation data also imply diversity of conformational transitions in different timescales near the *Phe*-ring patch.

As pointed out above, in the EphA2tm dimer interface there is a weekly polar cavity formed by Gly^{553} and Val^{554} residues and adjacent to the *Phe*-ring patch. The volume of the cavity depends on the conformational state of Phe^{557} side chains, with larger cavity corresponding to the *trans* rotamer of Cα-Cβ bond of Phe^{557} residues from both dimeric subunits. In the ^{15}N–edited TOCSY-HSQC spectrum, weak crosspeak on the water frequency was registered for the Phe^{556} amide group resonance corresponding to one from multiple local conformations of the C-terminal part of the TM dimer (Fig. S6 *B*) that indicates a water penetration into the EphA2tm dimer interface. Indeed, MD relaxation of the representative NMR structures in the explicit hydrated lipid DPPC bilayer demonstrated that up to four water molecules are capable of filling the weekly polar cavity depending on the mutual disposition of Phe^{556} and Phe^{557} side chains (Fig. 3 *D* and Fig. S6 *E*). These water molecules participate in the formation of a network of transient hydrogen bonds connecting the dimer subunits. Nevertheless, the existence of the vacant cavity in the dimeric interface can indicate a possibility of intermolecular interactions of the EphA2 TM domain with other membrane contents on which this cavity will be filled.

The conformational exchange revealed by NMR data and detailed out by the MD relaxation occurs on different timescales, from pico-nanosecond to micro-millisecond range. Thus, we observe a complex dynamic picture of the local conformational transitions in the C-terminal part of the EphA2tm dimer. Nevertheless, the locally increased ^{15}N{^{1}H}NOE values of Gly^{553}, Val^{554}, Phe^{556}, and Ile^{558} (Figs. 2 *F* and 3 *C*) indicate high local rigidity of the backbone chain of the TM helices near the phenylalanine rings on the pico-nanosecond timescale that can be a consequence of their π-π stacking interactions restricting sideways mobility around the water-accessible cavity. Indeed, despite the conformational switching of the aromatic interactions in the *Phe*-ring patch, simultaneous existence of multiple π-π and π-cation contacts might result in a significant stabilization of the local and global structure of the EphA2tm dimer. Furthermore, the conformational exchange of Phe^{557} side chain accompanied by numerous π-π and π-cation interactions having close enthalpy contributions might partially compensate for entropy decrease caused by immobilization of the bulk aliphatic side chains of Leu^{535}, Ile^{538}, Val^{543}, Val^{545}, Val^{546}, Leu^{549}, and Val^{550} during TM helix association. Thus, whereas the principal force meditating the EphA2tm dimerization is van der Waals packing in the knobs-into-holes manner, the C-terminal part of the dimer is stabilized by numerous aromatic interactions. These findings confirm the facts that aromatic residues are involved in specific TM helix-helix recognition and that the π-π and π-cation interactions may contribute significantly to the TM helix association (45).

Aromatic phenylalanine and histidine residues have a strong propensity to face phospholipids in the headgroup region and are thought to act as anchors for a membrane protein (43). Because seven of nine human EphA receptors (Fig. S8) have both aromatic and basic residues at the C-terminal part of TM segment, the observation of π-π and π-cation interactions in the EphA2 TM dimer interface may indicate their importance for proper EphA receptor functioning. The structural connections between TM and juxtamembrane domains remain undecided. It is obvious that interactions between the residues located at the membrane interface on both edges of the TM domain provide these interconnections, and probably aromatic interactions play an essential role in the domain coupling. The existence of some diseases, associated with point mutations of aromatic or basic residues at the C-termini of TM helices of membrane proteins (46), indirectly confirms this assumption. It was shown recently that the amino acid substitutions in the C-terminal juxtamembrane region can modulate dimerization of TM domains of receptor tyrosine kinases (47).

DISCUSSION

Dimerization mode diversity of the Eph TM domains and a mechanism of the receptor activation

Besides the pattern of the extended heptad repeat motif $L^{535}X_3G^{539}X_2A^{542}X_3V^{546}X_2L^{549}$ that was found to be responsible for left-handed dimerization of EphA2tm, there is at least one potential characteristic dimerization tandem GG4-like motif $A^{536}X_3G^{540}X_3G^{544}$ (the so-called ''glycine zipper'' (48)) located on the lipid-exposed surface of the EphA2tm dimer in the N-terminal part of the TM helix (Fig. 3, *B*, *D*, and *E*). Notably, both dimerization motifs are connected by their weak polar surfaces near the N-terminus of the TM helix. Similar motif was recently shown (16) to be used in lipid bicelles for right-handed dimerization (at angle $\theta \sim -45^\circ$) of the TM domains of EphA1 (Fig. S5 *B*), another representative of the same family of receptors. Importantly, an alternative self-association of the EphA1tm presumably via a second C-terminal dimerization motif implying a left-handed crossing of TM helices at a small angle was also detected (unfortunately, without determination of the high-resolution dimeric structure) (16). Both left- and right-handed variants of dimerization appear to be quite common for TM helix packing of integral proteins, and the observed helix crossing angles of 15° and -45° are close to the most frequently occurring angles for parallel helix-helix interactions in membrane (49). In contrast with EphA2tm, the right-handed dimeric structure of EphA1tm was stable in the thin DMPC bilayer during MD energy relaxation. Interestingly, both receptors have the same length of the TM helical region (Fig. S8), ~38 Å (25 amino acids), but significantly smaller crossing angle between EphA2tm helices makes the dimeric structure ~3 Å longer. Thus, it can be suggested that the EphA2 TM domain would prefer thick or thin lipid bilayer on dimerization via different motifs resulting in the left- or right-handed conformations with extended or shortened overall dimer shape, respectively (Fig. 3 *G*). Nevertheless, both EphAtm fragments were successfully incorporated into identical lipid bicelles. This supports the idea that lipid bicelles are capable of minimizing hydrophobic mismatch with the solute protein by adaptation to its overall shape, whereas the membrane is less plastic, imposing spatial limitations on TM domain of a protein (40,50).

The described dimerization modes of the TM domains of EphA1 and EphA2 receptors represent an instructive example of the diversity of TM domain formation of receptor tyrosine kinases and can provide an explanation for the molecular mechanism of the Eph-ephrin signaling. Existence of alternative dimerization motif suggests a possibility for the EphA2 TM domain to be involved in additional helix-helix interactions with other partners (e.g., on heterodimerization or higher-order oligomerization) and/or a capability of the homodimer to switch between left- and right-handed dimerization modes. Indeed, in the case of the EphA1tm embedded in lipid bicelles we were observing slow transitions between the two alternatively packed dimers (16). Ligand-induced receptor dimerization or reorientation of monomers in the preformed receptor dimers are believed to be common mechanisms of receptor tyrosine kinase activation (8). Accumulating evidences suggest that both ephrins and Eph receptors are loosely preclustered in the plasma membrane, forming low-affinity ephrin-ephrin and Eph-Eph dimers, and that ephrin docking may cause an Eph receptor rearrangement, triggering aggregation into larger Eph-ephrin clusters (2,5,6,12,13). Hence, it seems quite likely that the switching between the two dimerization modes presumed for TM domains of EphA1 and EphA2 can represent a transition from inactive to active form of the receptor, implying that the so-called rotation-coupled activation mechanism (10,11) proposed for other families of receptor tyrosine kinases may take place during the Eph receptor signaling. The mechanism intends active involvement of TM domains in dimerization and activation of the receptor via proper helix-helix packing and rearranging. Although the Eph TM segments reveal relatively low amino acid sequence homology, several dimerization motifs, including at least one explicit GG4-like motif, can be identified in each Eph TM region (Fig. S8). The specific helix-helix interactions between Eph TM domains would impose certain restrictions on the allowable conformational transitions undergone by the full length receptor on its activation. Therefore, TM domains of the Eph receptors can play an important role during intercellular signal transduction across membrane, providing a leverage for underlying conformational transition and extra specificity for the receptor dimerization, clustering, and subsequent activation.

Possible membrane preferences of alternative dimerization modes of the Eph TM domains

The nature and duration of Eph receptor-ephrin signals are modulated by cell surface turnover of Eph-receptor complexes (2,12). Moreover, both Eph receptors and ephrins are localized and sorted into membrane microdomains rich in cholesterol, sphingolipids, and specific lipids known as lipid rafts, which may fuse together into larger signaling platforms on Eph receptor-ephrin binding (2,5,7,12,51). In addition, it was found that receptor tyrosine kinases, including Eph family receptors, are concentrated and highly organized in caveolae, a subclass of rafts, which are characterized by flask-like invaginations of the plasma membrane (52). We believe the available evidence supports an important role of the lipid raft clustering in the initiation, propagation and maintenance of Eph signal transduction events. In the recent study on EphA1 TM domain we have shown that the membrane composition, namely the presence of anionic lipids, can affect dimerization of the TM domain (16) and the entire activity of the EphA1 receptor. The finding that alternative dimerization modes of EphA2 TM domain apparently favor lipid bilayers of different thickness (Fig. 3, *B* and *G*, and Fig. S5) implies that the dimerization state of the TM domain can be affected by the thickness of surrounding membrane.

Results from a number of investigations have pointed out that the composition of lipid membrane and the hydrophobic matching between the hydrophobic thickness of lipid bilayer and the hydrophobic length of TM proteins are important physical properties that regulate lipid-protein and protein-protein interactions in biomembranes (40,41,53–55). Rafts are thicker than nonraft phase in lipid bilayer systems, as shown by both atomic force microscopy (56) and x-ray diffraction (57). The specific helix-helix interactions require precise mutual orientation of TM helices, imposing certain restrictions on their tilt angle and tilt direction, therefore proper hydrophobic matching in different lipid phases may influence the specific TM helix association (40,41). Activity of the Eph receptor can vary depending on its localization in the cellular membrane, e.g., in lipid rafts, etc. Hence, Eph signaling may be different from inside and outside these membrane microdomains, which can impart stability of certain dimeric conformation of the Eph TM domain, sorting proper oligomerization state of the receptor. Furthermore, a protein-induced bilayer distortion could be coupled with a bilayer deformation due to one or several other proteins and this could result in indirect lipid-mediated protein-protein lateral association in the membrane (40). Therefore, certain conformation of the TM domain, e.g., the one corresponding to the active state of the receptor, can initiate formation of bigger rafts with large ephrin-Eph signaling clusters within the plasma membrane. There might be certain synergy between activation of the signaling complex and local lipid composition and physical properties of the membrane.

Overall, we believe our findings imply that the membrane is apparently more than just a passive platform for integration of all participants of a signal transduction process through Eph receptors. Therefore, specific membrane properties in the vicinity of Eph receptors along with various intermolecular lipid-protein and protein-protein interactions of their TM domains within plasma membrane have to be taken into account in the development of actual models of Eph receptor-ephrin signaling complexes. Because elevated EphA2 receptor expression is associated with many types of human cancers (17,18), deciphering the underlying mechanisms of the Eph-ephrin signal transduction will not only help us to understand basic biological processes, but may also provide a novel form of cancer therapy by means of specifically inhibiting lateral association of the Eph TM domains in the plasma membrane.

SUPPORTING MATERIAL

Eight figures and one table are available at http://www.biophysj.org/biophysj/supplemental/S0006-3495(09)01732-9.

This work was supported by the Russian Foundation for Basic Research, Program MCB RAS, the Russian Federal Agency of Science and Innovations (SS-1061.2008.4), and the Russian Funds Investment Group.

REFERENCES

1. Kullander, K., and R. Klein. 2002. Mechanisms and functions of Eph and ephrin signaling. *Nat. Rev. Mol. Cell Biol.* 3:475–486.
2. Pasquale, E. B. 2005. Eph receptor signaling casts a wide net on cell behavior. *Nat. Rev. Mol. Cell Biol.* 6:462–475.
3. Lackmann, M., and A. W. Boyd. 2008. Eph, a protein family coming of age: more confusion, insight, or complexity? *Sci. Signal.* 1:re2.
4. Eph Nomenclature Committee. 1997. Unified nomenclature for Eph family receptors and their ligands, the ephrins. *Cell.* 90:403–404.
5. Blits-Huizinga, C. T., C. M. Nelersa, …, D. J. Liebl. 2004. Ephrins and their receptors: binding versus biology. *IUBMB Life.* 56:257–265.
6. Wimmer-Kleikamp, S. H., P. W. Janes, …, M. Lackmann. 2004. Recruitment of Eph receptors into signaling clusters does not require ephrin contact. *J. Cell Biol.* 164:661–666.
7. Gauthier, L. R., and S. M. Robbins. 2003. Ephrin signaling: one raft to rule them all? One raft to sort them? One raft to spread their call and in signaling bind them? *Life Sci.* 281:211–225.
8. Schlessinger, J. 2000. Cell signaling by receptor tyrosine kinases. *Cell.* 281:211–225.
9. Tao, R. H., and I. N. Maruyama. 2008. All EGF(ErbB) receptors have preformed homo- and heterodimeric structures in living cells. *J. Cell Sci.* 121:3207–3217.
10. Moriki, T., H. Maruyama, and I. N. Maruyama. 2001. Activation of preformed EGF receptor dimers by ligand-induced rotation of the transmembrane domain. *J. Mol. Biol.* 311:1011–1026.
11. Fleishman, S. J., J. Schlessinger, and N. Ben-Tal. 2002. A putative molecular-activation switch in the transmembrane domain of erbB2. *Proc. Natl. Acad. Sci. USA.* 99:15937–15940.
12. Vearing, C. J., and M. Lackmann. 2005. "Eph receptor signaling; dimerization just isn't enough". *Growth Factors.* 23:67–76.
13. Himanen, J. P., N. Saha, and D. B. Nikolov. 2007. Cell-cell signaling via Eph receptors and ephrins. *Curr. Opin. Cell Biol.* 19:534–542.

14. Li, E., and K. Hristova. 2006. Role of receptor tyrosine kinase transmembrane domains in cell signaling and human pathologies. *Biochemistry*. 45:6241–6251.
15. Mackenzie, K. R. 2006. Folding and stability of alpha-helical integral membrane proteins. *Chem. Rev.* 106:1931–1977.
16. Bocharov, E. V., M. L. Mayzel, …, A. S. Arseniev. 2008. Spatial structure and pH-dependent conformational diversity of dimeric transmembrane domain of the receptor tyrosine kinase EphA1. *J. Biol. Chem.* 283:29385–29395.
17. Surawska, H., P. C. Ma, and R. Salgia. 2004. The role of ephrins and Eph receptors in cancer. *Cytokine Growth Factor Rev.* 15:419–433.
18. Wykosky, J., and W. Debinski. 2008. The EphA2 receptor and ephrinA1 ligand in solid tumors: function and therapeutic targeting. *Mol. Cancer Res.* 6:1795–1806.
19. Chakrabarti, P., and G. Khorana. 1975. A new approach to the study of phospholipid-protein interactions in biological membranes. Synthesis of fatty acids and phospholipids containing photosensitive groups. *Biochemistry.* 14:5021–5033.
20. Sattler, M., J. Schleucher, and C. Griesinger. 1999. Heteronuclear multidimensional NMR experiments for the structure determination of proteins in solution employing pulsed field gradients. *Prog. Nucl. Magn. Reson. Spectrosc.* 34:93–158.
21. Cavanagh, J., W. J. Fairbrother, …, N. J. Skelton. 2006. Protein NMR Spectroscopy: Principles and Practice, 2nd ed. Academic Press, San Diego, CA.
22. Keller, R. L. J. 2004. The Computer Aided Resonance Assignment Tutorial. CANTINA Verlag, Goldau, Switzerland.
23. Orekhov, V. Y., D. E. Nolde, …, A. S. Arseniev. 1995. Processing of heteronuclear NMR relaxation data with the new software DASHA. *Appl. Magn. Reson.* 9:581–588.
24. Daragan, V. A., and K. H. Mayo. 1997. Motional model analyses of protein and peptide dynamics using ^{13}C and ^{15}N NMR relaxation. *Prog. Nucl. Magn. Reson. Spectrosc.* 31:63–105.
25. Güntert, P. 2003. Automated NMR protein structure calculation. *Prog. Nucl. Magn. Reson. Spectrosc.* 43:105–125.
26. Zwahlen, C., P. Legault, …, L. E. Kay. 1997. Methods for measurement of intermolecular NOEs by multinuclear NMR spectroscopy: application to a bacteriophage λ N-peptide/boxB RNA complex. *J. Am. Chem. Soc.* 119:6711–6721.
27. Cornilescu, G., F. Delaglio, and A. Bax. 1999. Protein backbone angle restraints from searching a database for chemical shift and sequence homology. *J. Biomol. NMR.* 13:289–302.
28. Lindahl, E., B. Hess, and D. van der Spoel. 2001. GROMACS 3.0: a package for molecular simulation and trajectory analysis. *J. Mol. Model.* 7:306–317.
29. Hofmann, K., and W. Stoffel. 1993. TMbase—a database of membrane spanning proteins segments. *Biol. Chem. Hoppe Seyler.* 374:166.
30. Efremov, R. G., and G. Vergoten. 1995. Hydrophobic nature of membrane-spanning α-helical peptides as revealed by Monte Carlo simulations and molecular hydrophobicity potential analysis. *J. Phys. Chem.* 99:10658–10666.
31. Kabsch, W., and C. Sander. 1983. Dictionary of protein secondary structure: pattern recognition of hydrogen-bonded and geometrical features. *Biopolymers.* 22:2577–2637.
32. Koradi, R., M. Billeter, and K. Wüthrich. 1996. MOLMOL: a program for display and analysis of macromolecular structures. *J. Mol. Graph.* 14, 51–55, 29–32.
33. DeLano, W. L. 2002. The PyMOL Molecular Graphics System. DeLano Scientific, Palo Alto, CA.
34. Prosser, R. S., F. Evanics, …, M. S. Al-Abdul-Wahid. 2006. Current applications of bicelles in NMR studies of membrane-associated amphiphiles and proteins. *Biochemistry.* 45:8453–8465.
35. Bocharov, E. V., Y. E. Pustovalova, …, A. S. Arseniev. 2007. Unique dimeric structure of BNip3 transmembrane domain suggests membrane permeabilization as a cell death trigger. *J. Biol. Chem.* 282:16256–16266.
36. Bocharov, E. V., K. S. Mineev, …, A. S. Arseniev. 2008. Spatial structure of the dimeric transmembrane domain of the growth factor receptor ErbB2 presumably corresponding to the receptor active state. *J. Biol. Chem.* 283:6950–6956.
37. Luchette, P. A., T. N. Vetman, …, J. Katsaras. 2001. Morphology of fast-tumbling bicelles: a small angle neutron scattering and NMR study. *Biochim. Biophys. Acta.* 1513:83–94.
38. Andersson, A., and L. Mäler. 2005. Magnetic resonance investigations of lipid motion in isotropic bicelles. *Langmuir.* 21:7702–7709.
39. Langosch, D., and J. Heringa. 1998. Interaction of transmembrane helices by a knobs-into-holes packing characteristic of soluble coiled coils. *Proteins.* 31:150–159.
40. Nyholm, T. K., S. Ozdirekcan, and J. A. Killian. 2007. How protein transmembrane segments sense the lipid environment. *Biochemistry.* 46:1457–1465.
41. Sparr, E., W. L. Ash, …, J. A. Killian. 2005. Self-association of transmembrane alpha-helices in model membranes: importance of helix orientation and role of hydrophobic mismatch. *J. Biol. Chem.* 280:39324–39331.
42. Nagle, J. F., and S. Tristram-Nagle. 2000. Structure of lipid bilayers. *Biochim. Biophys. Acta.* 1469:159–195.
43. Adamian, L., V. Nanda, …, J. Liang. 2005. Empirical lipid propensities of amino acid residues in multispan alpha helical membrane proteins. *Proteins.* 59:496–509.
44. Unterreitmeier, S., A. Fuchs, …, D. Langosch. 2007. Phenylalanine promotes interaction of transmembrane domains via GxxxG motifs. *J. Mol. Biol.* 374:705–718.
45. Johnson, R. M., K. Hecht, and C. M. Deber. 2007. Aromatic and cation-pi interactions enhance helix-helix association in a membrane environment. *Biochemistry.* 46:9208–9214.
46. Bakker, M. J., J. G. van Dijk, …, M. A. Tijssen. 2006. Startle syndromes. *Lancet Neurol.* 5:513–524.
47. Peng, W. C., X. Lin, and J. Torres. 2009. The strong dimerization of the transmembrane domain of the fibroblast growth factor receptor (FGFR) is modulated by C-terminal juxtamembrane residues. *Protein Sci.* 18:450–459.
48. Kim, S., T.-J. Jeon, …, J. U. Bowie. 2005. Transmembrane glycine zippers: physiological and pathological roles in membrane proteins. *Proc. Natl. Acad. Sci. USA.* 102:14279–14283.
49. Walters, R. F. S., and W. F. DeGrado. 2006. Helix-packing motifs in membrane proteins. *Proc. Natl. Acad. Sci. USA.* 103:13658–13663.
50. Lind, J., J. Nordin, and L. Mäler. 2008. Lipid dynamics in fast-tumbling bicelles with varying bilayer thickness: effect of model transmembrane peptides. *Biochim. Biophys. Acta.* 1778:2526–2534.
51. Paratcha, G., and C. F. Ibáñez. 2002. Lipid rafts and the control of neurotrophic factor signaling in the nervous system: variations on a theme. *Curr. Opin. Neurobiol.* 12:542–549.
52. Wu, C., S. Butz, …, R. G. Anderson. 1997. Tyrosine kinase receptors concentrated in caveolae-like domains from neuronal plasma membrane. *J. Biol. Chem.* 272:3554–3559.
53. Marsh, D. 2008. Protein modulation of lipids, and vice-versa, in membranes. *Biochim. Biophys. Acta.* 1778:1545–1575.
54. Vidal, A., and T. J. McIntosh. 2005. Transbilayer peptide sorting between raft and nonraft bilayers: comparisons of detergent extraction and confocal microscopy. *Biophys. J.* 89:1102–1108.
55. de Meyer, F. J., M. Venturoli, and B. Smit. 2008. Molecular simulations of lipid-mediated protein-protein interactions. *Biophys. J.* 95:1851–1865.
56. Lawrence, J. C., D. E. Saslowsky, …, R. M. Henderson. 2003. Real-time analysis of the effects of cholesterol on lipid raft behavior using atomic force microscopy. *Biophys. J.* 84:1827–1832.
57. Gandhavadi, M., D. Allende, …, T. J. McIntosh. 2002. Structure, composition, and peptide binding properties of detergent soluble bilayers and detergent resistant rafts. *Biophys. J.* 82:1469–1482.